Structure and Activity of (2,8)-Dicarba-(3,12)-cystino α-ImI, an α-Conotoxin Containing a Nonreducible Cystine Analogue†

Christopher A. MacRaild,‡ Jayamini Illesinghe,§ Bianca J. van Lierop,§ Amanda L. Townsend,|| Mary Chebib,⊥ Bruce G. Livett,|| Andrea J. Robinson,§ and Raymond S. Norton‡,*

The Walter and Eliza Hall Institute of Medical Research, 1G Royal Parade, Parkville 3050, Victoria, Australia, School of Chemistry, Monash University, Clayton 3800, Victoria, Australia, Department of Biochemistry and Molecular Biology, Bio21 Institute, University of Melbourne, Parkville 3010, Australia, Faculty of Pharmacy, The University of Sydney, Sydney, NSW 2006, Australia

Received September 14, 2008

The α-conotoxins are potent and selective antagonists of nicotinic acetylcholine receptors (nAChR). Exploitation of these and other peptides in research and clinical settings has been hampered by the lability of the disulfide bridges that are essential for toxin structure and activity. One solution to this problem is replacement of cystine bridges with nonreducible dicarba linkages. We explore this approach by determining the solution structure and functional characteristics of a dicarba analogue of the α-conotoxin α-ImI, (2,8)-dicarba-(3,12)-cystino α-ImI. The structure of the dicarba analogue was similar to that of native α-ImI, with differences attributable to the different covalent geometry of the disulfide and dicarba bridges. Dicarba-α-ImI maintained inhibitory activity of nAChR comparable to that of native α-ImI in two in vitro assays. These findings confirm the potential of the dicarba linkage to improve stability while maintaining α-conotoxin function.

Conotoxins are venom peptides produced by marine snails of the genus *Conus*.[1,2] They represent a rich and diverse source of bioactive agents with highly specific activities and as such have attracted considerable attention as possible lead compounds in the development of novel therapeutics.[3] The α-conotoxins, in particular, show promise as therapeutic and neurochemical tools, being subtype-specific antagonists of nicotinic acetylcholine receptors (nAChR[a]). α-Conotoxins are peptides of 12−18 residues, containing two strictly conserved disulfides that are essential to toxin structure and function. However, these disulfides are a potential impediment to the exploitation of α-conotoxins, as they may limit metabolic stability[4] and place significant constraints on production, formulation, and storage.

The replacement of disulfide linkages with more stable alternatives has long been regarded as an attractive strategy to alleviate these problems. In particular, the replacement of the S−S motif of the cystine bridge with carbon atoms (in the form of CH_2-CH_2 or CH=CH groups) has been achieved in a number of disulfide-bridged hormones and other bioactive peptides.[5−12] In many of these cases, biological function has been maintained[5,7−11] and several show improved pharmacokinetic properties.[6,10] Until recently, however, this approach has been synthetically challenging. The application of microwave assisted ring-closing metathesis to this problem has resulted in a general, simple, and highly efficient strategy for dicarba incorporation in the context of a conventional solid-phase peptide synthesis.[12]

An important issue, which is likely to influence the success of this approach in specific situations, arises from the significant differences in covalent geometry between the disulfide and dicarba bridges. The carbon−sulfur and sulfur−sulfur bonds of cystine are substantially longer than the equivalent carbon−carbon bonds in the dicarba linkage as a consequence of the larger radius of the sulfur atom. In addition, the dihedral angle about the disulfide bond is strongly constrained to values near ±100°,[13] a conformation that is not readily approximated by either the saturated or unsaturated dicarba bridge. The implications of these differences in geometry for the structure and function of a given peptide are challenging to predict. Here we explore this question experimentally by determining the solution structure of (2,8)-dicarba-(3,12)-cystino α-ImI and by assessing the capacity of this analogue to antagonize nAChRs. The extensive structural and functional data available for native α-ImI[14−17] permit a detailed examination of the structural consequences of the dicarba substitution and afford a rationalization of the observed functional data.

Experimental Procedures

Peptide Synthesis. Synthesis of unsaturated (2,8)-dicarba-(3,12)-cystino α-ImI (dicarba-ImI) was achieved by microwave-assisted ring closing metathesis of L-allylglycine (Agl) residues, as described previously.[12] Briefly, the precursor linear peptide was prepared by Fmoc solid-phase peptide synthesis on rink amide resin to yield *C*-terminally amidated peptide. Agl was incorporated in place of Cys at positions 2 and 8 of the α-ImI sequence to facilitate the cyclization reaction. On-resin ring-closing metathesis proceeded quantitatively after 1 h of continuous microwave irradiation at 60 W, maintaining a temperature of 100 °C in the presence of 20 mol % second-generation Grubb's catalyst in dichloromethane containing 10% 0.4 M LiCl/DMF. Following cleavage from the resin and 2,2′-dipyridyl disulfide catalyzed oxidation of the remaining disulfide linkage, the product was purified by RP-HPLC and analyzed by mass spectroscopy as described.[12]

† Assigned chemical shifts, experimental restraints and structures have been deposited with the BioMagResBank database with accession number 20033.

* To whom correspondence should be addressed. Phone: +61 3 9345 2306. Fax: +61 3 9345 2686. E-mail: ray.norton@wehi.edu.au.

‡ The Walter & Eliza Hall Institute of Medical Research.

§ Monash University.

|| University of Melbourne.

⊥ University of Sydney.

[a] Abbreviations: dicarba-ImI, (2,8)-dicarba-(3,12)-cystino α-ImI; Agl, L-allylglycine; Δ4Das, 2,7-diaminodehydrosuberic acid (2,7-diaminooct-4-enedioic acid); DQF-COSY, double-quantum filtered correlation spectroscopy; nAChR, nicotinic acetylcholine receptor; NOESY, nuclear Overhauser effect spectroscopy; rmsd, root mean squared deviation; RP-HPLC, reverse phase high performance liquid chromatography; TOCSY, total correlation spectroscopy.

10.1021/jm8011504 CCC: $40.75
Published on Web 01/06/2009

Functional Assays. Adrenal chromaffin cells were isolated from adult bovine adrenal glands as described.[18] Isolated cells were plated out on collagen-coated 24-well plates at a density of 2.8×10^5 cells/cm^2. Four-day-old cultured chromaffin cells were equilibrated to room temperature for 5 min and washed twice in Locke's buffer (154 mM NaCl, 2.6 mM KCl, 2.15 mM K_2HPO_4, 0.85 mM KH_2PO_4, 10 mM D-glucose, 1.18 mM $MgSO_4 \cdot 7H_2O$, 2.2 mM $CaCl_2 \cdot 2H_2O$, 0.5% BSA, pH 7.4) for 5 min. Cells were then incubated for 5 min with 0.2−10 μM of the various α-ImI analogues before stimulation with 4.0 μM nicotine for a further 5 min. The incubation mixture was separated from the cells and acidified with 2.0 M perchloric acid to give a final concentration of 0.4 M perchloric acid. The catecholamines remaining in the cells were released by lysing the cells with 0.01 M perchloric acid and then acidified by addition of an equal volume of 0.8 M perchloric acid. Precipitated proteins were removed by centrifugation at 16000 rcf for 10 min. To measure basal release of catecholamines, a control well contained Locke's buffer only, with no nicotine or test compound. To determine the maximal release of catecholamines, a second control well contained nicotine (4 μM) but no test compound (i.e., no conotoxin or analogue). Catecholamines present in each sample were separated by RP-HPLC with a Waters HPLC system and C18 150 mm × 4.6 mm column, 5 μm particle size (Bio-Rad, USA), using an isocratic elution of the mobile phase (10% methanol 70 mM KH_2PO_4, 0.1 mM NaEDTA, 0.2% heptane sulfonic acid). Catecholamines eluting from the column were identified by their retention time and quantified by electrochemical detection (650 mV BAS model LC-3A) with reference to known standards of adrenaline and noradrenaline.

α-Conotoxin ImI and the two dicarba α-ImI isomers were also evaluated as antagonists of rat α7 nAChRs expressed in *Xenopus* oocytes using two-electrode voltage clamp methods as described previously.[19] Rat α_7 nAChR cDNA was linearized with *Sma*I. Linearized cDNA was transcribed to mRNA using the T7 "mMESSAGE mMACHINE" kit (Ambion Inc. Austin, TX). In brief, oocytes were harvested from *Xenopus laevis* and defolliculated. The oocytes were then stored in ND96 solution (96 mM NaCl, 2 mM KCl, 1 mM $MgCl_2$, 1.8 mM $CaCl_2$, 5 mM HEPES) supplemented with 2.5 mM sodium pyruvate, 0.5 mM theophylline and 50 μg/mL gentamycin. Stage V−VI oocytes were injected with 10 ng/nL of mRNA and then stored at 16 °C. Recordings of receptor activity were obtained after two to four days by a two-electrode voltage clamp by means of a Geneclamp 500 amplifier (Axon Instruments Inc., Foster City, CA), a MacLab 2e recorder (AD Instruments, Sydney, NSW), and Chart version 5.5.6 program. Oocytes were voltage clamped at −60 mV using glass electrodes filled with 3 mM KCl (0.5−1.5 MΩ). The preparation was continually perfused with ND96 solution at room temperature. α-ImI (2.5 μM) and dicarba-ImI (2.5 μM) were applied for 3 min prior to application of ACh (300 μM) in the presence of the conotoxins. Doses of ACh alone (300 μM) were applied as controls at 15 min intervals to allow complete recovery of response. The effect of the conotoxins was evaluated against ACh (300 μM) and reported as a % inhibition of response.

NMR Spectroscopy. Samples were prepared for NMR by dissolving lyophilized peptide in 95% H_2O/5% ^2H_2O to a final peptide concentration of 10 mM. A series of one-dimensional spectra was collected at pH 2.9 and 5.9 and at temperatures of 5, 10, 15, 20, and 25 °C. Two-dimensional homonuclear TOCSY spectra with a spin-lock time of 60 ms, NOESY spectra with mixing times of 50, 100, 250, and 350 ms, and DQF-COSY spectra were recorded at pH 5.9 on Bruker DRX-600 and Avance 800 spectrometers. A 250 ms NOESY spectrum recorded at pH 5.9 and 15 °C was used for resonance assignments and NOE intensity measurements. Two dimensional homonuclear E-COSY and 250 ms mixing time NOESY spectra were acquired in 100% ^2H_2O, pH 6.3 (uncorrected) at 15 °C. Spectra were processed using TopSpin, version 1.3, and analyzed using XEASY, version 1.3.13.[20,21] $^1H-^{13}C$ HSQC and $^1H-^{13}C$ HMQC-TOCSY spectra for the assignment of ^{13}C chemical shifts and a $^1H-^{15}N$ HSQC spectrum for the assignment of ^{15}N chemical shifts were acquired at 15 °C on a Bruker Avance 500 spectrometer equipped with a TXI cryoprobe. Chemical shifts are presented in Table S1 in Supporting Information.

Structure Calculations. Distance constraints were calculated from the volumes of NOESY cross-peaks at 15 °C, pH 5.9, and 800 MHz. $^3J_{HNH\alpha}$ values were measured from a DQF-COSY spectrum and converted to φ dihedral restraints as follows: $^3J_{HNH\alpha} > 8$ Hz, $\varphi = -120 \pm 40°$; $^3J_{HNH\alpha} < 6$ Hz, $\varphi = -60 \pm 30°$. χ^1 angles were determined where possible by analyzing NOESY spectra with a short mixing time of 100 ms and $^3J_{H\alpha H\beta}$ values measured from the E-COSY spectrum.[22] Intensities of NOE cross-peaks measured in XEASY were calibrated using the CALIBA macro from the program CYANA.[23] Initial structures were calculated using torsion angle dynamics and simulated annealing protocols in CYANA, and structures were optimized for a low target function. These structures were used to identify hydrogen bond partners for backbone amide protons that had temperature coefficients less negative than −4.6 ppb/K, indicative of protection from the solvent.[24,25] Where such an amide formed a bond with the same partner in ≥80% of the CYANA structures, this hydrogen bond was included as a restraint in the later rounds of structure calculations. For each hydrogen bond constraint, upper limits of 2.4 and 3.3 Å were used for the distances from acceptor to proton and donor nitrogen atom to acceptor, respectively. These initial structures were also used to resolve the assignments of a number of ambiguous NOE cross-peaks. The final constraint set was then used to calculate a new family of 100 structures using conventional simulated annealing protocols in XPLOR-NIH.[26] The resulting structures were then further refined by restrained energy minimization in explicit solvent, and the 20 lowest energy structures were selected for analysis. In all structure calculations, the dicarba bridge was modeled as two α-amino butyric acid residues, each with two H^γ atoms removed and a $C^\beta-C^\gamma-H^\gamma$ angle of 120°. For initial calculations in CYANA, distance restraints were applied of 1.34 Å for the $C^\gamma-C^\gamma$ distance and 2.5 Å for the $C^\gamma-C^\beta$ distance across the dicarba bridge. Force constants for these restraints were 10 times those applied to experimental distance restraints. For subsequent calculations in XPLOR-NIH, the covalent $C^\gamma-C^\gamma$ double bond was modeled explicitly, with trigonal-planar geometry about C^γ, a 1.34 Å bond length, and the standard covalent force constants of the XPLOR-NIH protein force-field. Analysis of the resulting structural ensembles was performed using the programs MOLMOL[27] and PROCHECK.[28] Figures were prepared with MOLMOL[27] and PYMOL.[29]

Results

Peptide Synthesis. Unsaturated (2,8)-dicarba-(3,12)-cystino α-ImI (dicarba-ImI) was synthesized and purified by preparative RP-HPLC, as shown in Figure 1. Two isomers of the expected mass were resolvable by RP-HPLC, presumably representing the cis and trans configurations of the dicarba double bond, respectively (see below).

Dicarba-ImI is a nAChR Antagonist. The capacity of α-ImI to antagonize nicotinic acetylcholine receptors was assessed in two in vitro functional assays. In the first, primary monolayer cultures of bovine adrenal chromaffin cells were stimulated with nicotine, and catecholamine release was taken as a measure of nAChR function. The ability of the dicarba-ImI isomers to inhibit catecholamine release was compared to that of native α-ImI in a dose−response study. Consistent with previous results, native α-ImI inhibits catecholamine release from these cells in a dose-dependent fashion. Both isomers of dicarba-ImI were found to similarly inhibit catecholamine release, albeit with a potency 10−20 fold lower than that of native α-ImI (Table 1, Supporting Information Figure S1).

As reported previously,[30] α-ImI was a potent competitive inhibitor of the homomeric α7 neuronal nAChR. Therefore, the activity of both isomers of dicarba-ImI was also assessed on

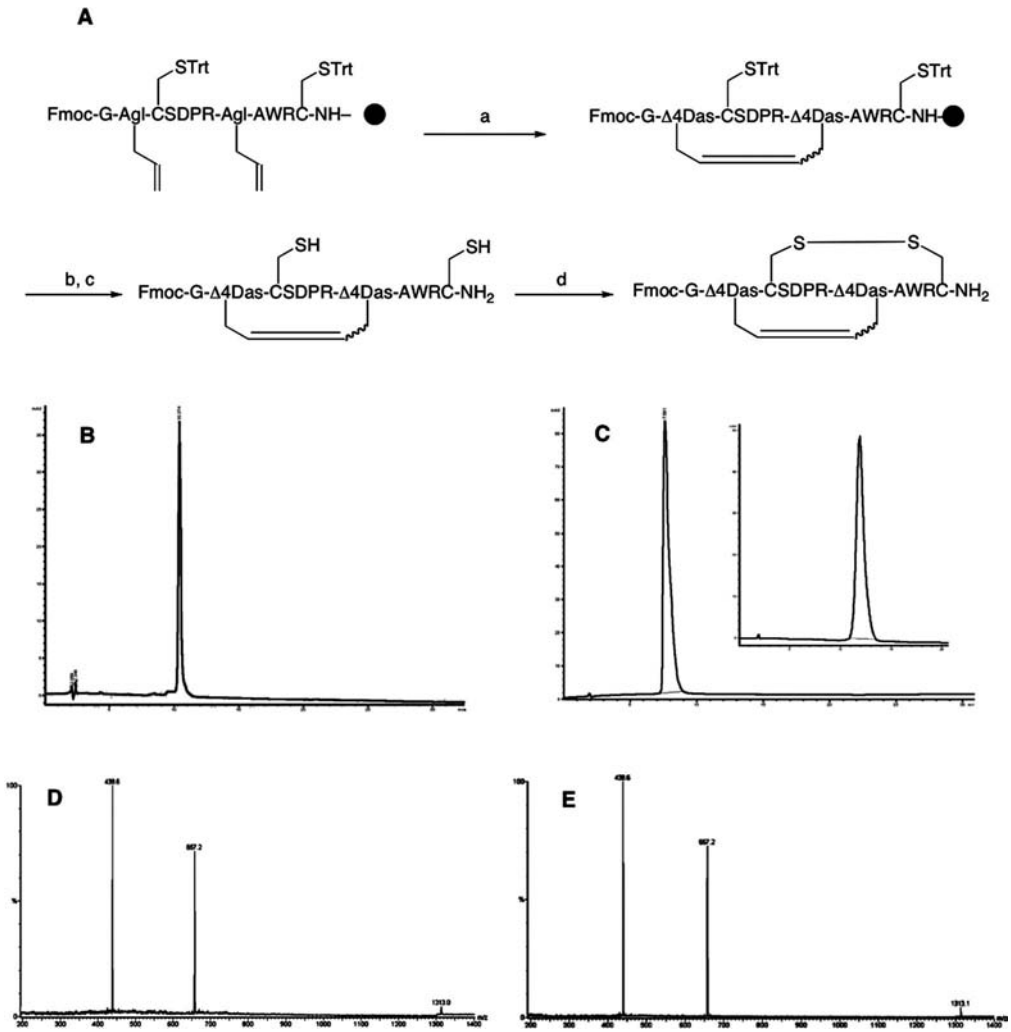

Figure 1. Reagents and conditions (A): Rink amide resin (●, 0.52 mmol g^{-1} loading); (a) 20 mol% second generation Grubbs' catalyst, DCM:0.4 M LiCl in DMF (90:10), rt → 100 °C, 1 h, 60 W of microwave irradiation; (b) 20% piperidine in DMF, rt, 20 min; (c) TFA:TIPS:H_2O:anisol (95:2:2:1), rt, 4 h; (d) 2,2′-dipyridyl disulfide, 0.1% aqueous TFA, rt, 10 min. RP-HPLC and ESI-MS analysis of dicarba-ImI analogues: isomer I (RP-HPLC trace, rt) (B); isomer II (RP-HPLC trace, heated column (50 °C), inset (RP-HPLC trace, rt)) (C); isomer I (ESI-MS) (D); isomer II (ESI-MS) (E).

Table 1. Inhibition of Nicotine-Stimulated Catecholamine Release

	IC_{50} of noradrenaline release (μM)[a]	IC_{50} of adrenaline release (μM)[a]
α-ImI	0.87 ± 0.04	1.12 ± 0.08
dicarba-ImI isomer I	17 ± 12	10 ± 2
dicarba-ImI isomer II	20 ± 15	15 ± 1

[a] Best-fit IC_{50} values ± standard error ($n = 4$).

frog oocytes expressing rat α7 nAChR. Figure 2 shows the effect of α-ImI and its dicarba analogues on ACh-evoked ion currents in frog oocytes expressing the α7 nAChR. Peptides were tested at 2.5 μM on the frog oocytes expressing rat α7 nAChR. Dicarba-ImI isomer I (2.5 μM) did not activate the receptor when applied alone but in the presence of ACh (300 μM) inhibited the response by 60 ± 9% ($n = 3$). Similarly, α-ImI (2.5 μM) did not activate the receptor when applied alone but in the presence of ACh (300 μM) inhibited the response by 68 ± 10% ($n = 3$). Thus, the inhibitory activity of isomer I at 2.5 μM was identical to that of native α-ImI. In contrast, dicarba-ImI isomer II was inactive at 2.5 μM (data not shown).

The apparent discrepancy between these results reflects the different nAChR subtypes involved. Chromaffin cells are known to express a number of nAChR subtypes, but those responsible for catecholamine release under our experimental conditions are unknown. In an assay essentially identical to that employed here, nicotine-stimulated catecholamine release from chromaffin cells was not sensitive to α-bungarotoxin, indicating that α7 nAChRs are not involved.[31]

NMR Spectroscopy. The two isomers of dicarba-ImI isolated by RP-HPLC were first examined by one-dimensional ^{1}H NMR. The spectra of isomer I showed that it adopted a unique folded conformation under all solution conditions examined (Supporting Information Figure S2). A single pair of olefinic resonances confirmed the presence of the unsaturated dicarba bridge and confirmed the homogeneity of the sample with respect to the conformation about the dicarba double bond. There was also no evidence of proline cis−trans isomerization in this sample. In contrast, isomer II showed evidence of multiple conformational or chemical states, with the major set of NMR resonances comprising approximately 60% of the total signal (Supporting Information Figure S3). Despite significant effort, we were unable to further purify isomer II. NOESY spectra of isomer II showed cross-peaks attributable to conformational exchange, most notably between major and minor peaks of the single Trp indole NH resonance (Supporting Information Figure S4). This

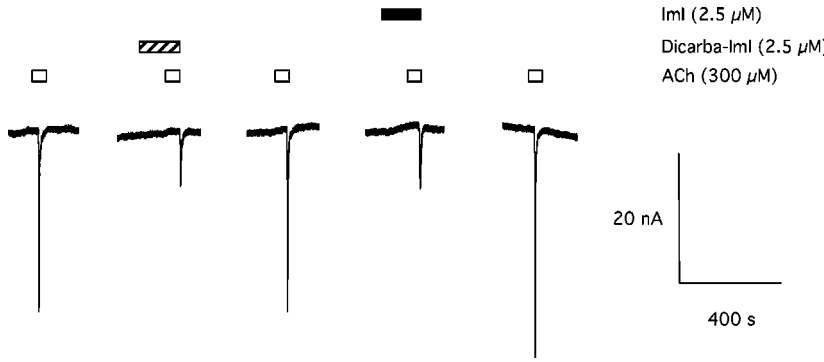

Figure 2. Effect of α-ImI and its dicarba analogues on ACh-evoked ion currents in frog oocytes expressing α7 nAChRs. ACh (300 μM) (duration indicated by open bar) activates oocytes expressing human α_7 nACh receptors clamped at −60 mV. Dicarba-ImI [isomer I] (2.5 μM; duration 3 min indicated by the hatched bar) did not activate the receptor when applied alone but inhibited the response in the presence of ACh (300 μM). Similarly, α-ImI (2.5 μM; duration 3 min indicated by the black bar) did not activate the receptor when applied alone but inhibited the response in the presence of ACh (300 μM).

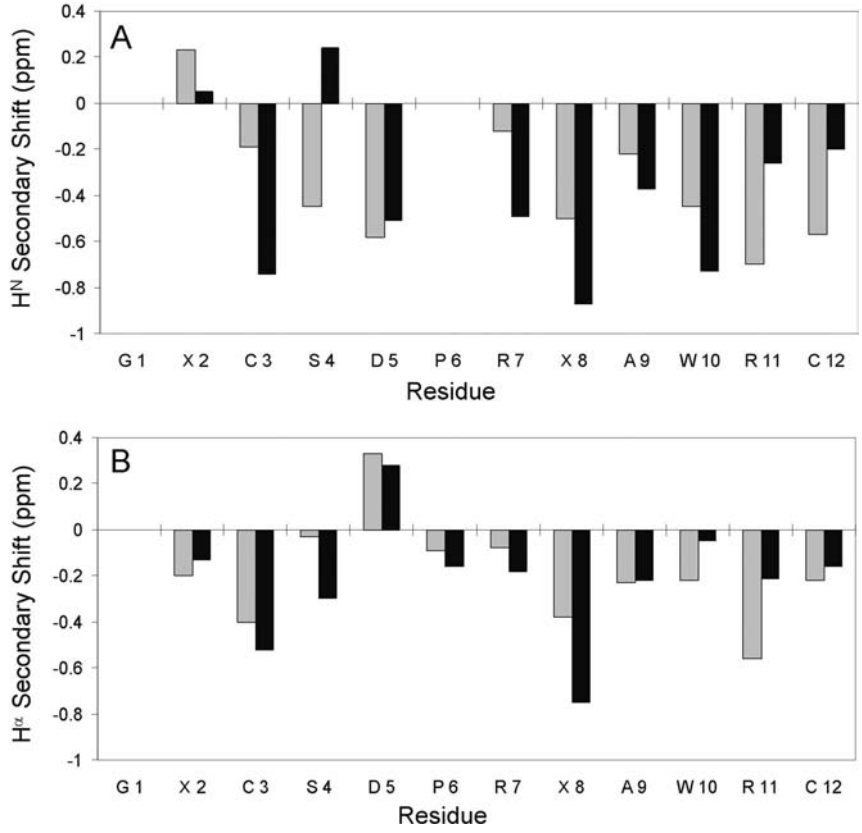

Figure 3. Secondary chemical shifts of the NH (A) and H^α (B) resonances of dicarba-ImI at 15 °C and pH 5.9 (black) compared to those reported for native α-ImI at 15 °C and pH 2.9[17] (gray).

observation suggests that the observed heterogeneity may be attributed at least in part to the existence of multiple conformational states in exchange on a subsecond time scale. The presence of conformational heterogeneity in our isomer II preparations was further supported by the significant temperature-dependent broadening of its RP-HPLC elution peak (Figure 1). For this reason, all further structural analysis focused on isomer I.

To assign isomers I and II to the cis and trans dicarba isomer, respectively, we attempted to quantify the scalar coupling across the dicarba bridge. For isomer I, this proved challenging because of the very similar chemical shifts of the two H^γ atoms and couplings to their respective H^β resonances. The major H^γ peaks of isomer II, on the other hand, were slightly better resolved, and showed the characteristic doublet asymmetry of strong scalar coupling for $^3J_{H^\gamma-H^\gamma}$; this permitted an estimation of $^3J_{H^\gamma-H^\gamma}$ for isomer II of approximately 15 Hz (Supporting Information Figure S5). On this basis, we assign isomer II as the trans dicarba isomer.

Sequence-specific chemical shift assignments for backbone and side chain protons were made by conventional analysis of two-dimensional homonuclear NMR spectra. The amide resonance of residue 2 was broadened by exchange with solvent and was only evident in one-dimensional ^1H spectra at low pH or low temperature. The H^α resonances of Gly1 could not be identified unambiguously; although candidate peaks were evident in 1D spectra at 3.87, 3.90, and 3.92 ppm (15 °C and pH 5.9), these were not adequately resolved in 2D spectra to permit unambiguous assignment. Reported chemical shifts for Gly1 H^α of α-ImI are 3.82, 3.87 (25 °C and pH 3.0),[17] and 3.95 (7 °C

Table 2. Summary of Experimental Constraints and Structural Statistics for Dicarba-ImI

No. of Conformational Restraints		
total no. of distance restraints	103	
intraresidue ($i = j$)	39	
sequential ($\|i - j\| = 1$)	33	
medium-range ($1 < \|i - j\| < 5$)	18	
long-range ($\|i - j\| > 4$)	13	
hydrogen bond restraints	2	
no. of dihedral restraints	9	
Energies[a]	cis[b]	trans[c]
E_{NOE} (kcal mol^{-1})	9.8 ± 1.2	19.3 ± 3.9
$E_{dihedral}$ (kcal mol^{-1})	0.02 ± 0.01	0.2 ± 0.6
rms Deviations from Experimental Data		
NOEs (Å)	0.04 ± 0.002	0.06 ± 0.005
dihedrals (deg)	0.03 ± 0.01	0.03 ± 0.02
Deviations from Ideal[d]		
angles (deg)	0.6 ± 0.1	0.64 ± 0.04
bonds (Å)	0.0035 ± 0.0001	0.0044 ± 0.0003
impropers (deg)	0.57 ± 0.01	0.37 ± 0.03
Atomic rms Deviations (Å)[e]		
all heavy atoms	0.88	0.87
backbone heavy atoms, residues 2−12	0.20	0.28
Ramachandran Plot[f]		
most favored (%)	53.9	36.1
allowed (%)	34.4	44.4
additionally allowed (%)	11.7	19.4
disallowed (%)	0	0

[a] The values for E_{NOE} are calculated from a square well potential with force constants of 30 kcal mol^{-1} Å^{-2}. [b] Structures calculated with dicarba bridge constrained in cis conformation. [c] Structures calculated with dicarba bridge constrained in trans conformation. [d] The values for the bonds, angles, and impropers show the rms deviations from ideal covalent geometry as defined by the XPLOR forcefield. [e] The average rmsd to the mean as calculated in MOLMOL. [f] As reported by PROCHECK-NMR for all residues.

and pH 3.1).[32] ^{1}H,^{13}C, and ^{15}N assignments for dicarba-ImI at 15 °C and pH 5.9 are tabulated in Supporting Information (Table S1) and deposited in BioMagResBank with accession number 20033. Figure 3 compares the deviations of the backbone NH and H$^\alpha$ chemical shifts from random coil values for dicarba and native α-ImI.[17]

Structural Restraints. Restraints on the torsion angle φ were derived for Ser4 and Δ4Das8 (2,7-diaminodehydrosuberic acid; the residue corresponding to one-half of the dicarba bridge) ($^3J_{HNH\alpha} > 8$ Hz, $\varphi = -120 \pm 40°$) and Cys3, Ala9, and Trp10 ($^3J_{HNH\alpha} < 6$ Hz, $\varphi = -60 \pm 30°$). Side chain χ^1 torsion angles determined from intraresidue NOEs and $^3J_{H\alpha H\beta}$ values were 60 ± 60° for Cys3, 180 ± 60° for Asp5, and 60 ± 60° for Trp10.[22] An additional dihedral restraint was applied to the torsion angle about the dicarba double bond. The force constant applied to this restraint was ramped over the cooling phase of the calculations to a final value equal to that of the improper restraints in the default XPLOR force field. Because we were not able to unambiguously resolve the ^3J coupling across this bond in isomer I, this restraint maintained either a cis or trans configuration about this bond in alternate structure calculations. The results of these calculations identified the cis configuration as the one most consistent with the available experimental constraints derived from isomer I, as detailed below. This finding is consistent with our assignment of isomer II as the trans isomer and our expectation that the two isolated isomers differ in the configuration of the dicarba double bond.

Attempts to derive torsion angle restraints from chemical shifts using TALOS[33] and PREDITOR[34] failed to yield high-confidence predictions that were consistent between the two approaches and supported by other experimental restraints. This failure is probably the result of a number of factors, including the absence of carbonyl chemical shift data, the influence of the dicarba substitution on chemical shifts, and the fact that these torsion angle prediction algorithms are trained and validated against globular proteins with more extensive regular secondary structure than is present in a small conotoxin such as α-ImI.

We identify a strong H$^\alpha$−H$^\delta$ NOE between residues 5 and 6, which confirms a trans configuration for the peptide bond preceding Pro6 in dicarba-ImI. This is identical to the reported conformation for the equivalent bond in α-ImI.[17]

Backbone amide temperature coefficients less negative than −4.6 ppb/K were observed for Arg7 and Δ4Das8 (Supporting Information Table S2) and were taken to indicate the involvement of these groups in hydrogen bonds.[24,25] On the basis of initial structure calculations, we identified the hydrogen bond acceptor for Arg7 as the side chain carboxyl of Asp5, and the acceptor for Δ4Das8 as the backbone carbonyl of Asp5. Identical hydrogen bonds are observed in the NMR structure of native α-ImI.[17] A total of 103 nonredundant distance restraints derived from assigned NOESY cross-peaks was included in the final structure calculations, as summarized in Table 2. Of these NOEs, 13 involved the olefinic protons of the dicarba bridge, including six medium-range NOEs between the dicarba bridge and residues 5, 10, and 11.

Solution Structure of Dicarba-ImI. Two sets of structure calculations for dicarba-ImI were run in parallel, assuming either cis or trans configuration of the dicarba double bond. Parameters characterizing the final 20 structures for each calculation are summarized in Table 2. Energy terms corresponding to the experimental restraints were systematically higher in the ensemble of trans structures and the Ramachandran statistics were worse, implying that the cis configuration was more consistent with the experimentally derived restraints. Further analysis therefore focused on the structural ensemble calculated assuming a cis dicarba bridge. This ensemble of structures shows excellent agreement with the experimental restraints and correct covalent geometry. The Ramachandran plot shows reasonable backbone stereochemical quality, comparable to those in published solution structures of α-ImI (Table 2). Indeed, the solution structure of α-ImI has been well characterized, with at least five NMR structures published.[17,32,35−37] A recent comparison of these structures with that of the closely related α-conotoxin α-RgIA[38] identified the structure of Rogers et al. (1IM1)[17] as the most representative of the available solution structures. The following analysis of the dicarba-ImI structure will therefore use PDB entry 1IM1 as the principal point of comparison for the structure of the native toxin.

The family of structures of dicarba-ImI is shown in Figure 4, superimposed with the solution structure ensemble of native α-ImI.[17] The overall fold of dicarba-ImI closely resembles that of the native toxin, although some differences are clearly evident. The structures of α-conotoxins are typically characterized in terms of the conformations of the two disulfide-defined loops. In the case of α-ImI, loop I corresponds to residues 3−8 while loop II corresponds to residues 9−12. Table 3 shows average backbone rmsd between the dicarba-ImI ensemble and the closest-to-average structure of native α-ImI. It is evident that the backbone conformations of the two loops are very similar in the two structures, as the rmsd between dicarba-ImI and the native toxin is only slightly greater than the mean pairwise rmsd within the dicarba-ImI ensemble. The principal difference between the two structures is thus the orientation of

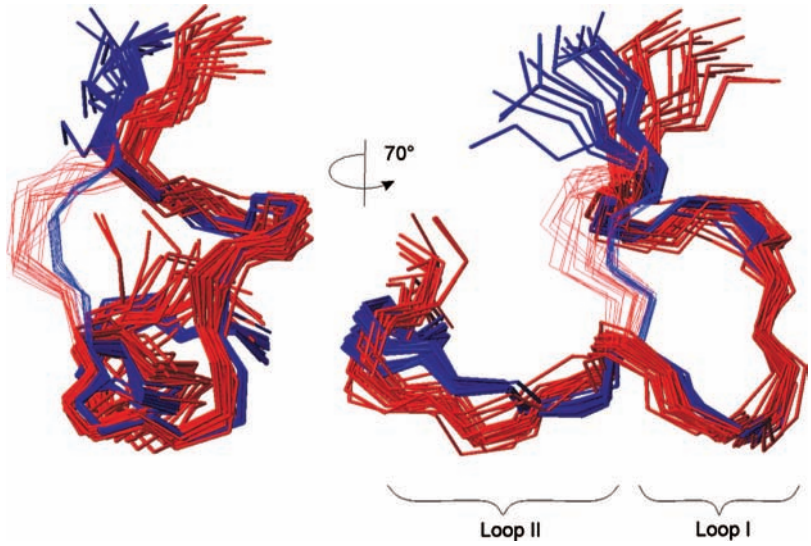

Figure 4. Comparison of the backbone conformation of dicarba-ImI (blue) and native α-ImI (PDB 1IM1) (red). The 2,8 dicarba and disulfide linkages are shown as blue and red lines, respectively.

Table 3. Backbone Atomic rms Deviations

	loop I[a]	loop II[b]	loop I + loop II[c]
dicarba-ImI[d]	0.11 ± 0.06	0.12 ± 0.07	0.25 ± 0.13
dicarba-ImI vs 1IM1[e]	0.41 ± 0.03	0.38 ± 0.02	1.1 ± 0.1

[a] Residues 3−8. [b] Residues 9−12. [c] Residues 3−12. [d] Pairwise rmsd over the dicarba-ImI ensemble of structures. [e] rmsds between a representative structure of α-ImI (model 3 of 1IM1) and the dicarba-ImI ensemble.

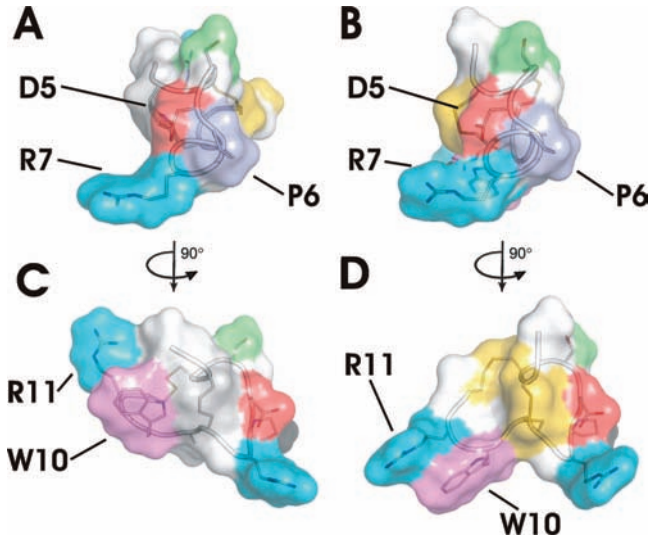

Figure 5. Solvent-accessible surface representations of the structure of dicarba-ImI (A,C) and native α-ImI (B,D). Side chain surfaces are colored by residue type, as follows: Arg, blue; Asp, red; Cys, yellow; dicarba bridge, gray; Pro, purple; Ser, green; Trp, magenta.

the loops with respect to each other. This is further emphasized by comparison of surface representations of the dicarba and native ImI structures (Figure 5). The conformation of loop I (facing the reader in Figure 5A,B) adopts an almost identical conformation in the two structures. Likewise, loop II adopts a similar conformation, but its orientation with respect to the rest of the molecule differs significantly (Figure 5C,D). This difference in loop orientation is a consequence of subtle changes in backbone conformation at residue 8 and results in a slightly more compact structure for the dicarba form of the toxin. Direct experimental support for this more compact conformation comes from a number of long-range NOEs from the sidechains of residues 10 and 11 to the dicarba and disulfide bridges. This orientation of loop II effectively closes the cleft formed between the two disulfide bridges and Trp10 in the native α-ImI structure[17] (Figure 5).

A second point of structural difference between the native and dicarba forms of α-ImI is the orientation of the two N-terminal residues, once again the result of a localized change in backbone conformation but this time centered at residue 2. This disrupts the hydrogen bond between the carbonyl of Gly1 and the amide of Ser4 seen in the native toxin structure. It is striking that the two significant differences in backbone structure between dicarba-ImI and the native form are centered at residues 2 and 8, the two residues participating in the dicarba bridge. The observed structural differences are thus a direct consequence of the different covalent geometry of the dicarba bridge as compared to the disulfide. To illustrate the implications of this difference in geometry, consider the distance between the C^{β} atoms involved in the linkage. In the case of the unsaturated dicarba bridge, this distance is expected to be tightly constrained by the planarity of the double bond, and indeed it is 2.94 ± 0.01 Å in the ensemble of dicarba-ImI structures. The equivalent distance in the solution structure of α-ImI is 3.7 ± 0.2 Å, and in the complex with Ac-AChBP,[39] it is 3.99 Å. Clearly, such significant variations in this distance cannot occur without changes in backbone conformation.

Discussion

To better understand the functional consequences of the structural features described above, we have compared the ensemble of calculated structures of dicarba-ImI with the crystal structure of the complex of α-ImI with the *Aplysia californica* acetylcholine binding protein (Ac-AChBP), a soluble homologue of the ligand binding domain of the nAChR.[39] The structure of α-ImI in this complex is very similar to the solution structure of Rogers et al.[17] The most important contacts between α-ImI and the nAChR, as identified by extensive mutagenesis, involve residues Asp5, Pro6, and Arg7 of α-ImI interacting with the principal face of the ACh binding site.[14−16] The equivalent interactions are maintained when the solution structure of dicarba-ImI is superimposed on the structure of the native toxin bound to Ac-AChBP (Figure 6A,B). The conformation of this

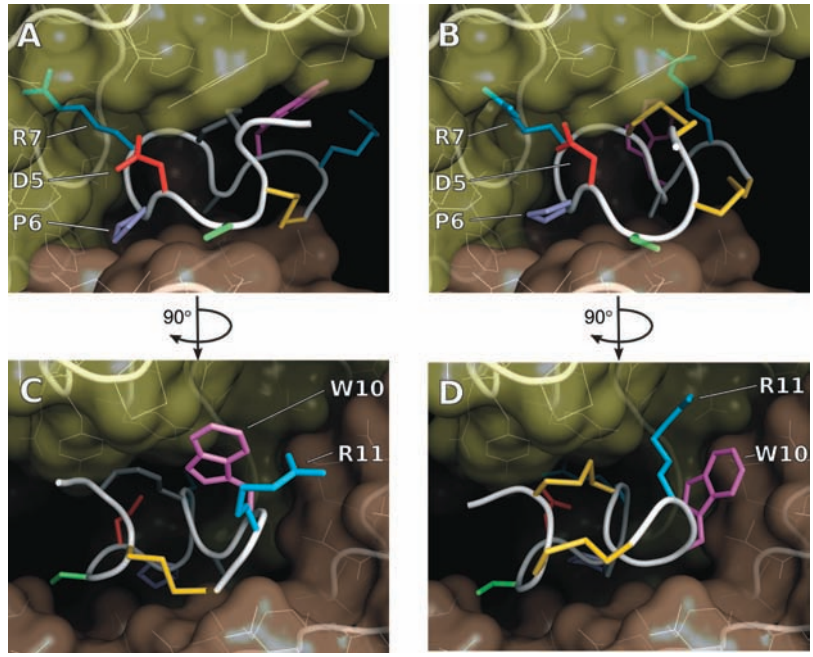

Figure 6. Model of the interaction of dicarba-ImI with *Aplysia californica* AChBP (A,C) and the crystal structure of native α-ImI bound to *A. californica* AChBP (PDB ID 2BYP) (B,D). The model complex was generated by superimposing the closest-to-average dicarba-ImI structure on the C^{α} atoms of residues 2−12 of the native toxin in the crystal structure. The principal (+) face of the binding protein is yellow and the complementary (−) face is brown. α-ImI side-chains are colored by residue type using the same colors as Figure 5.

tripeptide motif is strongly constrained by two hydrogen bonds between the side chain carboxyl and backbone carbonyl of Asp5 and the backbone amides of Arg7 and Cys8, respectively. The presence of these hydrogen bonds in dicarba-ImI is demonstrated by the temperature coefficients of these amide protons.

Additional contacts, which appear to be less critical determinants of the α-ImI/nAChR interaction, involve Trp10 of α-ImI and residues of the complementary face of the binding pocket. These interactions are disrupted in the modeled dicarba-ImI/Ac-AChBP complex, owing to the closed conformation of loop II in dicarba-ImI (Figure 6C,D). Similarly, a salt bridge between Arg11 and a glutamate residue on the principal face of the ACh binding site of Ac-AChBP is disrupted by the change in orientation of loop II. α-ImI activity against α7 nAChRs is highly tolerant of mutation at Arg11 and moderately tolerant of mutation at Trp10.[16] As such, the functional importance of these interactions is unclear in the native toxin. It may be significant, however, that the principal face of the ACh binding pocket is largely conserved across the nAChR subtypes, suggesting that determinants of subtype specificity reside in the complementary face-loop II interactions. Supporting this hypothesis are recent studies of the related α-conotoxin α-RgIA.[38] The sequence of α-RgIA differs from α-ImI only in the presence of an additional residue at the C terminus, and at residues 9 and 10, which are Arg and Tyr in α-RgIA in place of Ala and Trp in α-ImI. α-RgIA shows specificity for α9-containing nAChR subtypes, with only weak antagonistic activity against α7 receptors. The R9A mutant of α-RgIA inverts this specificity, being more active against α7 receptors than α9α10.[38] It remains to be determined whether the altered loop II conformation of dicarba-ImI significantly alters its receptor subtype specificity with respect to the native toxin. Finally, the closed conformation of loop II forces an alternate structure on the remaining 3−12 disulfide, such that residue 12 clashes with the guanidino group of R59 (residue numbering of 2BYP) on the complementary face of Ac-AChBP. The corresponding residue is not conserved among the nAChRs. For example, in the α7 nAChR subtype, the corresponding residue is serine, suggesting that this apparent steric clash is unlikely to significantly influence dicarba-ImI activity against mammalian nAChRs.

The results of this study emphasize the importance of relatively subtle changes in covalent geometry to the structure and activity of cystine-rich peptides. Although isomer I displayed similar activity against rat α7 nACh receptors to native α-ImI, it showed significant structural differences, which can be attributed to the covalent geometry of the dicarba bridge. On the other hand, isomer II, which differs from isomer I only in the configuration about the dicarba bridge, did not adopt a single stable conformation in solution. Nor did it show activity against rat α7 nAChR under the conditions of our assay, although it did show inhibitory activity in our chromaffin cell assay, suggesting that it may maintain activity against an as yet unidentified nAChR subtype.

The success of strategies involving the substitution of dicarba bridges for disulfides in bioactive peptides will be contingent on these effects and their implications in terms of the functional interactions of the peptide. Such effects are not amenable to simple generalization or reliable prediction and will require experimental testing on a system-by-system basis. It is noteworthy in this regard that recent synthetic developments[12] make possible the production and testing of numerous analogues of the dicarba bridge. In particular, analogues that increase the length or flexibility of the linkage may prove valuable in relieving the conformational strain apparently induced in dicarba-ImI. To this end, the unsaturated dicarba bridge may be hydrogenated to yield the saturated form, which is expected to possess greater flexibility. Alternatively, an additional methylene group might be inserted to yield a longer linkage.

Acknowledgment. We thank Gracia Quek and Helena Safavi-Hemami for research assistance. Rat α7 nACh receptor cDNA encapsulated in pBSSK(+) was a gift from Professor Jim Boulter (Neuropsychiatric Institute, University of California, Los Angeles). This work was supported in part by a grant from

the Australian Research Council (LP0774874). R.S.N. acknowledges fellowship support from the Australian National Health and Medical Research Council.

Supporting Information Available: Two tables containing assigned chemical shifts and amide temperature coefficients for dicarba-ImI, and seven figures showing the dose response of α-ImI and dicarba-ImI on nicotine-evoked adrenaline release from bovine adrenal chromaffin cells, ^{1}H NMR spectra of dicarba α-ImI isomer I and II, a NOESY spectrum showing exchange-derived cross peaks involving alternate conformational states of isomer II, ^{1}H 1D and DQF-COSY spectra of isomer II showing strong $^3J_{H\gamma-H\gamma}$ coupling across the dicarba bridge, representative NOESY and TOCSY spectra of isomer I and the ensemble of 20 structures determined for dicarba α-ImI. This material is available free of charge via the Internet at http://pubs.acs.org.

References

(1) Norton, R. S.; Olivera, B. M. Conotoxins down under. *Toxicon* **2006**, *48*, 780–798.

(2) Janes, R. W. α-Conotoxins as selective probes for nicotinic acetylcholine receptor subclasses. *Curr. Opin. Pharmacol.* **2005**, *5*, 280–292.

(3) Livett, B. G.; Gayler, K. R.; Khalil, Z. Drugs from the sea: conopeptides as potential therapeutics. *Curr. Med. Chem.* **2004**, *11*, 1715–1723.

(4) Armishaw, C. J.; Daly, N. L.; Nevin, S. T.; Adams, D. J.; Craik, D. J.; Alewood, P. F. α-Selenoconotoxins, a new class of potent α7 neuronal nicotinic receptor antagonists. *J. Biol. Chem.* **2006**, *281*, 14136–14143.

(5) Hase, S.; Morikawa, T.; Sakakibara, S. Synthesis of a biologically active analog of deamino-8-arginine-vasopressin which does not contain a disulphide bond. *Experientia* **1969**, *25*, 1239–1240.

(6) Oka, T.; Nakanishi, A.; Okada, T. Studies on pharmacological and biochemical properties of deamino-dicarba-[GLY-7]-oxytocin (Y-5350). *Jpn. J. Pharmacol.* **1975**, *25*, 15–24.

(7) Kambayashi, Y.; Nakajima, S.; Ueda, M.; Inouye, K. A dicarba analog of *β*-atrial natriuretic peptide (*β*-ANP) inhibits guanosine 3′,5′-cyclic monophosphate production induced by α-ANP in cultured rat vascular smooth muscle cells. *FEBS Lett.* **1989**, *248*, 28–34.

(8) Cerovský, V.; Wünsch, E.; Brass, J. Enzymatic semisynthesis of dicarba analogs of calcitonin. *Eur. J. Biochem.* **1997**, *247*, 231–237.

(9) Lange, M.; Cuthbertson, A. S.; Towart, R.; Fischer, P. M. Synthesis and activity of dimeric bradykinin antagonists containing diaminodicarboxylic acid bridge residues. *J. Pept. Sci.* **1998**, *4*, 289–293.

(10) Stymiest, J. L.; Mitchell, B. F.; Wong, S.; Vederas, J. C. Synthesis of biologically active dicarba analogues of the peptide hormone oxytocin using ring-closing metathesis. *Org. Lett.* **2003**, *5*, 47–49.

(11) Stymiest, J. L.; Mitchell, B. F.; Wong, S.; Vederas, J. C. Synthesis of oxytocin analogues with replacement of sulfur by carbon gives potent antagonists with increased stability. *J. Org. Chem.* **2005**, *70*, 7799–7809.

(12) Robinson, A. J.; Elaridi, J.; Van Lierop, B. J.; Mujcinovic, S.; Jackson, W. R. Microwave-assisted RCM for the synthesis of carbocyclic peptides. *J. Pept. Sci.* **2007**, *13*, 280–285.

(13) Richardson, J. S. The anatomy and taxonomy of protein structure. *Adv. Protein Chem.* **1981**, *34*, 167–339.

(14) Ellison, M.; McIntosh, J. M.; Olivera, B. M. α-Conotoxins ImI and ImII. Similar α7 nicotinic receptor antagonists act at different sites. *J. Biol. Chem.* **2003**, *278*, 757–764.

(15) Quiram, P. A.; Jones, J. J.; Sine, S. M. Pairwise interactions between neuronal α7 acetylcholine receptors and α-conotoxin ImI. *J. Biol. Chem.* **1999**, *274*, 19517–19524.

(16) Quiram, P. A.; Sine, S. M. Structural elements in α-conotoxin ImI essential for binding to neuronal α7 receptors. *J. Biol. Chem.* **1998**, *273*, 11007–11011.

(17) Rogers, J. P.; Luginbuhl, P.; Shen, G. S.; McCabe, R. T.; Stevens, R. C.; Wemmer, D. E. NMR solution structure of α-conotoxin ImI and comparison to other conotoxins specific for neuronal nicotinic acetylcholine receptors. *Biochemistry* **1999**, *38*, 3874–3882.

(18) Livett, B. G.; Mitchelhill, K. I.; Dean, D. M. Adrenal chromaffin cells—their isolation and culture. In *In Vitro Methods for Studying Secretion*; Elsevier Science Publishers BV, Biomedical Division: Amsterdam, 1987; pp 171−175.

(19) Barker, D.; Lin, D. H.; Carland, J. E.; Chu, C. P.; Chebib, M.; Brimble, M. A.; Savage, G. P.; McLeod, M. D. Methyllycaconitine analogues have mixed antagonist effects at nicotinic acetylcholine receptors. *Bioorg. Med. Chem.* **2005**, *13*, 4565–4575.

(20) Bartels, C.; Xia, T. H.; Billeter, M.; Güntert, P.; Wüthrich, K. The program XEASY for computer-supported NMR spectral-analysis of biological macromolecules. *J. Biomol. NMR* **1995**, *6*, 1–10.

(21) Doreleijers, J. F.; Mading, S.; Maziuk, D.; Sojourner, K.; Yin, L.; Zhu, J.; Markley, J. L.; Ulrich, E. L. BioMagResBank database with sets of experimental NMR constraints corresponding to the structures of over 1400 biomolecules deposited in the Protein Data Bank. *J. Biomol. NMR* **2003**, *26*, 139–146.

(22) Wagner, G.; Braun, W.; Havel, T. F.; Schaumann, T.; Go, N.; Wüthrich, K. Protein structures in solution by nuclear magnetic resonance and distance geometry. The polypeptide fold of the basic pancreatic trypsin inhibitor determined using two different algorithms, DISGEO and DISMAN. *J. Mol. Biol.* **1987**, *196*, 611–639.

(23) Güntert, P. Automated NMR structure calculation with CYANA. *Methods Mol. Biol.* **2004**, *278*, 353–378.

(24) Baxter, N. J.; Williamson, M. P. Temperature dependence of 1H chemical shifts in proteins. *J. Biomol. NMR* **1997**, *9*, 359–369.

(25) Cierpicki, T.; Otlewski, J. Amide proton temperature coefficients as hydrogen bond indicators in proteins. *J. Biomol. NMR* **2001**, *21*, 249–261.

(26) Schwieters, C. D.; Kuszewski, J. J.; Tjandra, N.; Clore, G. M. The Xplor-NIH NMR molecular structure determination package. *J. Magn. Reson.* **2003**, *160*, 65–73.

(27) Koradi, R.; Billeter, M.; Wüthrich, K. MOLMOL: a program for display and analysis of macromolecular structures. *J. Mol. Graphics* **1996**, *14*, 51–55; 29−32.

(28) Laskowski, R. A.; Rullmannn, J. A.; MacArthur, M. W.; Kaptein, R.; Thornton, J. M. AQUA and PROCHECK-NMR: programs for checking the quality of protein structures solved by NMR. *J. Biomol. NMR* **1996**, *8*, 477–486.

(29) DeLano, W. L. *The PyMol Molecular Graphics System*; DeLano Scientific: Palo Alto CA, 2008.

(30) Johnson, D. S.; Martinez, J.; Elgoyhen, A. B.; Heinemann, S. F.; McIntosh, J. M. α-Conotoxin ImI exhibits subtype-specific nicotinic acetylcholine receptor blockade: preferential inhibition of homomeric α7 and α9 receptors. *Mol. Pharmacol.* **1995**, *48*, 194–199.

(31) Broxton, N. M.; Down, J. G.; Gehrmann, J.; Alewood, P. F.; Satchell, D. G.; Livett, B. G. α-Conotoxin ImI inhibits the α-bungarotoxin-resistant nicotinic response in bovine adrenal chromaffin cells. *J. Neurochem.* **1999**, *72*, 1656–1662.

(32) Gehrmann, J.; Daly, N. L.; Alewood, P. F.; Craik, D. J. Solution structure of α-conotoxin ImI by ^{1}H nuclear magnetic resonance. *J. Med. Chem.* **1999**, *42*, 2364–2372.

(33) Cornilescu, G.; Delaglio, F.; Bax, A. Protein backbone angle restraints from searching a database for chemical shift and sequence homology. *J. Biomol. NMR* **1999**, *13*, 289–302.

(34) Berjanskii, M. V.; Neal, S.; Wishart, D. S. PREDITOR: a web server for predicting protein torsion angle restraints. *Nucleic Acids Res.* **2006**, *34*, W63−69.

(35) Gouda, H.; Hirono, S. Solution structure of α-conotoxin ImI determined by two-dimensional NMR spectroscopy. *Biochim. Biophys. Acta* **1999**, *1431*, 384–394.

(36) Maslennikov, I. V.; Shenkarev, Z. O.; Zhmak, M. N.; Ivanov, V. T.; Methfessel, C.; Tsetlin, V. I.; Arseniev, A. S. NMR spatial structure of α-conotoxin ImI reveals a common scaffold in snail and snake toxins recognizing neuronal nicotinic acetylcholine receptors. *FEBS Lett.* **1999**, *444*, 275–280.

(37) Lamthanh, H.; Jegou-Matheron, C.; Servent, D.; Menez, A.; Lancelin, J. M. Minimal conformation of the α-conotoxin ImI for the α7 neuronal nicotinic acetylcholine receptor recognition: correlated CD, NMR and binding studies. *FEBS Lett.* **1999**, *454*, 293–298.

(38) Ellison, M.; Feng, Z. P.; Park, A. J.; Zhang, X.; Olivera, B. M.; McIntosh, J. M.; Norton, R. S. α-RgIA, a novel conotoxin that blocks the α9α10 nAChR: structure and identification of key receptor-binding residues. *J. Mol. Biol.* **2008**, *377*, 1216–1227.

(39) Hansen, S. B.; Sulzenbacher, G.; Huxford, T.; Marchot, P.; Taylor, P.; Bourne, Y. Structures of *Aplysia* AChBP complexes with nicotinic agonists and antagonists reveal distinctive binding interfaces and conformations. *EMBO J.* **2005**, *24*, 3635–3646.

JM8011504